LAWRENCE
LIVERMORE
NATIONAL
LABORATORY

LLNL-JRNL-736485

Hydrogen and Oxygen Stable Isotope Signatures of Goethite Hydration Waters by Thermogravimetry-Enabled Laser Spectroscopy

E. Oerter, M. Singleton, M. L. Davisson

August 9, 2017

Chemical Geology

Disclaimer

Hydrogen and Oxygen Stable Isotope Signatures of Goethite Hydration Waters by Thermogravimetry-Enabled Laser Spectroscopy

Erik Oerter[1]*, Michael Singleton[1], Lee Davisson[1]

[1] Lawrence Livermore National Laboratory, 7000 East Avenue, Livermore, CA 94550, USA.

* Corresponding Author email: erikjoerter@gmail.com

Keywords

Stable isotope hydrology, paleoclimatology, dehydroxylation, mineral-water fractionation, hydrous minerals

Highlights

TGA-IRIS system enables fast and precise $\delta^{2}H$ and $\delta^{18}O$ measurements of liquid samples and mineral hydration waters.

TGA-IRIS approach does not require laborious and hazardous sample processing.

TGA-IRIS enables the determination of Fe-OH $\delta^{18}O$ values and fractionation factors that have not been accessible until now

Abstract

The hydrogen and oxygen stable isotope composition ($\delta^{2}H$ and $\delta^{18}O$ values) of mineral hydration waters can give information on the environment of mineral formation. Here we present and validate an approach for the stable isotope analysis of mineral hydration waters

based on coupling a thermogravimetric analyzer with a laser-based isotope ratio infrared spectroscopy instrument (Picarro L-2130i), which we abbreviate as TGA-IRIS. TGA-IRIS generates δ^2H and $\delta^{18}O$ values of liquid water samples with precision for δ^2H of $\pm$ 1.2‰, and for $\delta^{18}O$ of $\pm$ 0.17‰. For hydration waters in goethite, precision for δ^2H ranges from $\pm$ 0.3‰ to 1.6‰, and for $\delta^{18}O$ ranges from $\pm$ 0.17‰ to 0.27‰. The ability of TGA-IRIS to generate detailed water yield data and δ^2H and $\delta^{18}O$ values of water at varying temperatures allows for the differentiation of water in varying states of binding on mineral surfaces and within the mineral matrix. TGA-IRIS analyses of hydrogen isotopes in goethite yields δ^2H values that reflect the hydrogen of the OH^- phase in the mineral and are comparable to that made by IRMS and found in the literature. In contrast, $\delta^{18}O$ values on goethite reflect the oxygen in OH^- groups bound to Fe (Fe-OH group), and not the oxygen bound only to Fe (Fe-O group) in the mineral crystal lattice, and may not be comparable to literature $\delta^{18}O$ values made by IRMS that reflect the total O in the mineral. TGA-IRIS presents the possibility to isotopically differentiate the various oxygen reservoirs in goethite, which may allow the mineral to be used as a single mineral geothermometer. TGA-IRIS measurements of hydration waters are likely to open new avenues and possibilities for research on hydrated minerals.

1. Introduction

The geochemistry of Earth's terrestrial environment is dominated by weathering reactions driven principally by the abundant presence of water and oxygen (e.g. Garrels and Christ, 1965; Maher and Chamberlain, 2014). This corrosive and oxidative environment results in the significant presence of hydrated mineral weathering products such as Fe oxide and phyllosilicate minerals across nearly all of Earth's surface (e.g. Cornell and Schwertmann, 2003; Nesbitt and Young, 1989; Yapp, 2001; and others). Hydrated mineral phases have also been observed on Mars, which suggests the presence of liquid water at the surface during Mars' past (Mustard et al., 2008).

Hydrated minerals may retain a signal of the environmental conditions under which they formed because their parent waters can be of meteoric origin and therefore have

climatologically distinct hydrogen and oxygen stable isotope compositions (e.g. Dansgaard, 1964; Lawrence and Taylor, 1971, 1972; Bowen, 2010), while their temperature of formation imparts systematic fractionation from the parent waters to the incorporated mineral-hydration water (Friedman and Oneil, 1977). Therefore, if the hydrogen and oxygen stable isotope compositions of the mineral-bound waters can be measured, information about the mineral formation environment can be understood (e.g. Savin and Epstein, 1970; Shepard and Gilg, 1996; Savin and Hsieh, 1998). Interpretations of paleoclimate conditions during Earth's history have been made based on analyses of hydrogen and oxygen stable isotopes of hydrated minerals found in the rock record, including that of phyllosilicates (e.g. Savin and Epstein, 1970; Shepard and Gilg, 1996; Savin and Hsieh, 1998; Feng and Yapp 2009) and Fe oxides (e.g. Yapp and Pedley, 1985; Yapp, 1987; Girard et al., 2000; Yapp, 2001; Yapp and Shuster, 2011).

An impediment to the more widespread application of hydrogen and oxygen stable isotope analyses of mineral hydration waters has been the complexity of liberating hydration water from the mineral matrix and analyzing it by mass spectrometry. Several approaches have been used, including thermal breakdown of goethite to hematite followed by quantitative conversion of the water to H_2 for isotopic analysis (Yapp and Pedley, 1985), chemical extraction of the total oxygen in hydrated minerals by fluorination (e.g. Clayton and Mayeda, 1963; Yapp, 1987), high-temperature (1450 °C) thermal decomposition to release mineral hydration water (Sharp et al., 2001; Rohrssen et al., 2008), and the use of incremental vacuum dehydration at varying temperatures (Yapp, 2015). Each requires subsequent conversion of hydrogen and oxygen to gaseous H_2 or CO_2 followed with analysis by gas-source isotope ratio mass spectrometry (IRMS). These methods are labor- and time-intensive, and require complex laboratory apparatus for off-line sample preparation.

The advent of laser-based isotope ratio infrared spectroscopy (IRIS) (Kerstel et al., 1999; Kerstel and Gianfrani, 2008) offers several advantages to IRMS analyses, most significantly that hydrogen and oxygen stable isotope values, and water vapor concentrations are measured simultaneously on the same sample of water vapor with no need to convert water to other gases. IRIS instruments are also lower cost and have reduced complexity compared to IRMS. IRIS instruments do require that a water sample be converted to vapor for sample induction,

and techniques to sample liquid water include quantitative vaporization (Gupta et al., 2009), direct liquid-vapor equilibration (Wassenaar et al., 2008; Koehler et al., 2013; Hendry et al., 2015), and membrane-inlet vapor equilibration (Munksgaard et al., 2011; Volkmann and Weiler, 2014; Rothfuss et al., 2013; Oerter et al., 2017a; Oerter et al., 2017b, Oerter and Bowen, 2017). For samples where water is incorporated into, or surrounded by a solid matrix (such as mineral hydration waters), the traditional approach is to first liberate the water from the sample using distillation by heat under vacuum (Araguas-Araguas et al., 1995; Orlowski et al., 2016). After water liberation, it is collected and introduced into the IRIS instrument by subsequent quantitative vaporization (Gupta et al., 2009). More recently, on-line techniques that produce water vapor from the sample by heating (Koehler and Wassenaar, 2012; Johnson et al., 2017; Cui et al., 2017) or microwave radiation (Munksgaard et al., 2014) have been developed, after which the water vapor is inducted directly into the IRIS instrument. A disadvantage of the currently available heat-based water liberation methods is that the sample is heated to a single high temperature and all of the sample's water is released in a single pulse. For samples that contain water in various states of binding strength (i.e. hydrated minerals) these water types will be mixed and analyzed together.

Thermogravimetric analysis (TGA) offers an attractive approach to the liberation of mineral-bound waters because the sample can be step-heated very precisely to isolate the release of waters of different binding strengths (i.e. lower temperatures for weakly-bound, higher temperature for strongly-bound), and the corresponding mass loss of water at each heating step can be precisely measured. In addition, the sample size required is very small (approximately 5-30 mg) and sample preparation is usually minimal. Recently, TGA has been utilized to liberate water vapor from hydrated clay minerals, which was collected by cryogenic trapping, and subsequently manually transferred and analyzed by IRIS (Yang et al., 2016).

Here we develop an on-line method utilizing a TGA instrument to liberate water vapor from liquid water samples and hydrated mineral samples, and transfer the vapor directly to an IRIS instrument where the hydrogen and oxygen stable isotope values of the water vapor are analyzed. We first show that the thermogravimetric analysis – isotope ratio infrared spectroscopy method (TGA-IRIS) can yield accurate and precise hydrogen and oxygen stable

isotope values from ~ sub μL-sized liquid water samples. We then apply the TGA-IRIS technique to synthetic and natural goethite samples to illustrate the novel applications of TGA-IRIS. We conclude that TGA-IRIS can contribute unique insights to the study of mineral hydration waters.

2. Experimental Methods

2.1 TGA-IRIS analytical system

A TA Discovery thermogravimetric analyzer (TGA) (TA Instruments, New Castle, DE, USA) with infrared-heated furnace and 25 position sample changer was connected to a Picarro L-2130i cavity ring down isotope ratio infrared spectroscopy (IRIS) water isotope analyzer (Picarro Inc., Santa Clara, CA, USA) by a heated sample transfer line. The IRIS inlet side of the sample transfer line is stainless steel tubing (1.6 mm O.D. x 0.6 mm I.D.) that is inserted 15 cm into stainless steel tubing (3.2 mm O.D. x 2.2 mm I.D.) attached to the TGA furnace outlet, thus forming an open split. The TGA-IRIS system is configured with this open-split interface between the TGA and the IRIS instrument to accommodate the greater N_2 carrier gas flow rates from the TGA compared to the induction flow rate of the IRIS instrument. The sample transfer line and open split is wrapped with resistance heating tape and temperature controlled to 80 °C.

Water vapor generated by sample heating in the TGA is carried through the system by N_2 carrier gas. Carrier N_2 flow rate was 25 mL min^{-1}, determined as the minimum flow rate that would prevent ambient atmospheric vapor from entering the open split, while minimizing dilution and travel time of the water vapor pulse carried from the TGA to the IRIS instrument.

2.2 TGA-IRIS analytical methods

Samples were loaded into pre-weighed (for tare correction in the TGA) sample holder pans (see Section 3.2 for details on encapsulating liquid water or wet samples), then loaded into the auto sampler. An initial weight loss with increasing heating temperature curve for unknown sample types was determined by heating at 10 °C min^{-1} from 35 to 600 °C, thus identifying water release temperature ranges of interest for subsequent TGA-IRIS analyses. In

order to generate sufficient H_2O vapor levels ($[H_2O]$ values in parts per million by volume, ppmV) in the IRIS instrument ($[H_2O]$ peak values > 5000 ppmV) for reliable measurement of δ values, water needs to be released from the sample quickly. Heating at a very fast rate of ≥5 °C sec^{-1} ("flash heating") to a temperature just higher than that needed to release the water from the sample is necessary. After flash heating, isothermal conditions are maintained at the desired temperature for 10 minutes to fully release the sample water available at that temperature so that there is no mixing between water yielded at subsequent temperatures. All heating schemes used in this study begin with an initial TGA furnace temperature of 35 °C for 5 minutes after sample loading and furnace closure to flush the system of ambient water vapor and return $[H_2O]$ values in the IRIS instrument to ≤ 250 ppmV before the rest of the heating scheme commences.

The IRIS instrument makes measurements of $[H_2O]$, and δ^2H and $\delta^{18}O$ values (in ‰ notation, see below) at approximately 1 Hz. Integration of the measured δ^2H and $\delta^{18}O$ values over the entire sample signal duration will yield quantitative δ^2H and $\delta^{18}O$ values of the water sample. The integrated δ^2H and $\delta^{18}O$ values were calculated with a weighted average of measured δ^2H and $\delta^{18}O$ values, with weighting factors for individual δ value measurements calculated as the ratio of the measured H_2O vapor concentration ($[H_2O]_{measured}$) of each 1 Hz measurement to the maximum H_2O vapor concentration ($[H_2O]_{max}$) for the sample. The start of the integration interval for each sample was initiated at the point that $[H_2O]_{measured}$ values increased above background (> 250 ppmV) and continued until $[H_2O]_{measured}$ values at the end of the H_2O vapor peak were < 2000 ppmV (Figure 1). Tests of varying the peak-end $[H_2O]$ cutoff value between 800 and 3000 ppmV did not yield large differences in δ^2H and $\delta^{18}O$ values, and thus 2000 ppmV was chosen as the value applied to all samples. However, we recommend that the peak-end $[H_2O]$ cutoff value by evaluated for the specific TGA-IRIS analytical system in use.

The presence of organic compounds in H_2O vapor has been shown to exert spectral interference and result in spurious δ values in IRIS analyses (West et al., 2010). To evaluate the potential presence of organics, several spectral parameters that the IRIS instrument records were evaluated for every analysis. The 'slope shift' and 'baseline shift' values reflect parameters in the spectral signal of the empty cavity during factory calibration, and 'residuals' reflects the

175 goodness of fit in that relationship (Munksgaard et al., 2014). Values of these three spectral
176 parameters during sample analyses were compared to that resulting from standard waters. No
177 organic contamination was detected in any of the samples in this study.
178

2.3 Standards and samples

Hydrogen and oxygen stable isotope values are reported in δ notation: δ = ($R_{sample}/R_{standard} - 1$), where R_{sample} and $R_{standard}$ are the $^{2}H/^{1}H$ or $^{18}O/^{16}O$ ratios for the sample and standards respectively, and values are reported in per mille (‰). Mineral-water fractionation factors ($\propto_{m-w}$) are calculated as: $\alpha = (R_{mineral}/R_{water})$.

Water used as standards (Table 1) were previously calibrated in our laboratory against the VSMOW2, SLAP2, and GISP primary standard reference materials using IRMS analysis. Measured TGA-IRIS $\delta^{2}H$ and $\delta^{18}O$ values were calibrated to the Vienna Standard Mean Ocean Water (VSMOW) standard (Coplen, 1994) by using run-specific linear correlations of known δ values to measured δ values from CHC, GTW, and NVW water standards (one of each) at the beginning and end of each analytical run (details in Section 2.3 below). Liquid water standards were also included at regular intervals through the runs to monitor for instrumental drift, though none was typically observed.

Synthetic goethite ("SynGoethite2") was prepared at room temperature (23 °C) by dissolving 1 molar Fe(III) from $FeCl_3$ in 2 molar HNO_3 and diluted with DI H_2O. NaOH was added to neutralize pH to between 7 and 9, iron-oxy-hydroxide precipitate was settled overnight, followed by centrifugation, decanting and dialysis until external water was <100 microSiemens, followed by air drying. SynGoethite2 was confirmed as goethite by x-ray diffraction (details below). The final $\delta^{2}H$ and $\delta^{18}O$ values of the water used to synthesize SynGoethite2 were -71.0‰ and -7.8‰ respectively. An aliquot of a natural sample of pure goethite (FCol-3) was provided by Dr. Crayton Yapp. FCol-3 is sourced from near Florissant, Colorado, USA and was confirmed as goethite by x-ray diffraction. Mineral samples were ground to a fine powder in a synthetic sapphire mortar and pestle with isopropyl alcohol, then treated with 0.5 M HCl at 23 °C and rinsed at least four times with deionized water. The samples were then treated with 30% H_2O_2 solution four times, after which the samples were rinsed several times with deionized water, and dried overnight at 40 °C.

Mineral compositions of the solid samples were determined by x-ray diffraction on a Bruker D8 Advance instrument (Bruker Corp., Billerica, MA, USA) using Cu-Kα radiation

generated at 40 kV and 40 mA. Diffraction scans were performed from 10-80° 2θ, with 0.02° 2θ step size with 2 sec collection time per step, with variable divergence slits.

3. Results and Discussion

To evaluate the accuracy, precision and utility of TGA-IRIS, we performed a series of experiments designed to test and constrain the performance of various aspects of the TGA-IRIS system. To facilitate the presentation of these activities and their results, in the following sections we describe each of the tests and discuss their results in sequence. We first show results on liquid water samples that demonstrate accuracy and precision limits of liquid water analyses. We then follow with results from synthetic and natural mineral samples of goethite.

3.1 Quantitative TGA-IRIS sample induction

To reliably analyze δ^2H and $\delta^{18}O$ values of the water vapor generated by the TGA, the sample vapor induction system must consistently capture the water vapor stream during every analysis. Figure 2 shows the relationship between the integrated sum of water vapor for each sample received at the IRIS instrument (in ppmV) and the liquid volume of 81 water samples ranging in volume from 400 to 1200 nL (volume calculated from sample mass loss measured by TGA; 1 mg = 1000 nL H_2O at 25 °C) for samples loaded in tin capsules (see Section 3.2 below) and flash heated to 150, 300, 450, and 600 °C (on separate aliquots). The strong correlations and similar slopes of the relationships between water vapor volume and liquid water volume for samples heated at 150 and 300 °C, (150 °C: slope = 2503, R^2 = 0.97, n = 31; 300 °C slope = 2200, R^2 = 0.97, n = 50) shown in Fig. 2 (data in Supp. Table 1) indicates that the TGA-IRIS system is consistently inducting the vapor generated from each sample flash heated to 150 and 300 °C in the TGA furnace. Therefore, calculating δ^2H and $\delta^{18}O$ values by a weighted average of each δ value weighted by its [H_2O] value as a proportion of the maximum [H_2O] value for each sample peak (as described in Section 2.2 above) is repeatable for samples heated at 150 and 300 °C. Liquid water samples heated to 450 and 600 °C show weaker vapor to liquid volume

relationships with lower slopes (450 °C: slope = 1463, R^2 = 0.12, n = 6; 600 °C: slope = 1638, R^2 = 0.90, n = 12) (Fig. 2), indicating more variability in vapor induction from liquid samples at those temperatures.

3.2 Effects of sample capsule material and heating temperature

The use of liquid water calibration standards introduced into the TGA furnace and therefore treated identically to the unknown samples presents some challenges for developing the proper procedure. Wet samples must be encapsulated to prevent evaporation of the sample (and thus alteration of δ^2H and $\delta^{18}O$ values), during sample loading and N_2 flushing of the TGA furnace before the analysis is begun. Tin or silver sample capsules are commonly available due to their use in various mass spectrometry techniques. Silver is often chosen for the high temperature (>1000 °C) thermal conversion analysis of water because it will not form oxides by reaction with H_2O under inert atmospheres. The degree to which silver's inert advantage is applicable to the lower temperatures of TGA-IRIS analysis is discussed below. Silver's disadvantages include reduced workability due to material hardness, higher cost, and reduced availability in the smallest capsule sizes. Tin capsules are easier to work with, available in very small size (1 mm diameter) that is suitable for sub-microliter liquid sample volumes, and are less costly.

Tin capsules (1.5 mm diam. x 5 mm length, Costech # 41064, n = 7) and silver capsules (2 mm diam. x 41075 5 mm length, EA # 41075, n = 7) were loaded with 600 (± 150) nL of either CHC or ATW liquid water by syringe injection, and sealed by crimping the top of the capsule closed with pliers, folding the crimp over itself and crimping again with pliers, forming a double-crimp seal. The isotopic effect of the water in the preexisting air headspace inside the capsule can be neglected because the liquid water added is ~1000x larger mass than that in the headspace air. These samples were analyzed by the TGA-IRIS method with a heating rate of 5 °C sec^{-1} ("flash-heated") from 35 to 300 °C, culminating in 10 minutes of isothermal conditions at 300 °C. Tin capsules yielded δ^2H values with a precision of ± 0.76‰ and $\delta^{18}O$ values of ± 0.13‰ (± 1σ (1 standard deviation) reproducibility, n=7), whereas silver capsules gave precision of ± 1.09‰ for δ^2H and ± 0.46‰ for $\delta^{18}O$ values (± 1σ, n=7). The silver capsules were

considerably more difficult to load and crimp, and these results do not include several silver capsule samples that gave null or dramatically high δ values, presumably because the water was not sufficiently contained in the capsule and either leaked out or evaporated before analysis. These problems were absent with the tin capsules.

After establishing that tin capsules were easier to work with and gave more reproducible results, it was necessary to assess whether tin capsule material reacts with water at TGA-IRIS temperatures to give spurious δ^2H or $\delta^{18}O$ values. Tin capsules (1.5 mm diam. x 5 mm length) were loaded with 800 ($\pm$ 180) nL of CHC liquid water, and double-crimp sealed. These samples were analyzed by TGA-IRIS and flash heated, culminating in 10 minutes of isothermal conditions at either 150, 300, 450, or 600 °C. This fast rate of heating was designed to match the heating rate needed to release adsorbed and structural water from solid samples (discussed in Section 3.6 below), thus satisfying the principle of identical treatment between samples and calibration standards.

Results of the heating experiments in measured δ^2H, $\delta^{18}O$ values (factory calibrated data) are shown in Fig. 3. No temperature dependence on measured δ^2H or $\delta^{18}O$ values was found ($R^2 < 0.2$ for both). We interpret the precision of measured δ values of liquid water samples at various temperatures to be as follows, based on $\pm 1\sigma$ of *n* measurements. For δ^2H, at 150 °C $\pm$ 1.23‰ *n* = 9, 300 °C $\pm$ 0.68‰ *n* = 8, 450 °C $\pm$ 0.62‰ *n* = 6, 600 °C $\pm$ 3.16‰ *n* = 9; and for $\delta^{18}O$, at 150 °C $\pm$ 0.17‰ *n* = 9, 300 °C $\pm$ 0.52‰ *n* = 8, 450 °C $\pm$ 0.87‰ *n* = 6, 600 °C $\pm$ 0.83‰ *n* = 9. Precision for δ^2H measurements is best in the 300 to 450 °C range, whereas $\delta^{18}O$ measurements are most precise at 150 °C, and decrease with increasing temperature (Fig. 3B). A possible reason for reduced precision for liquid water analyses at the highest temperatures is the reduction in quantitative sample induction in the 450 to 600 °C range (Fig. 2, Section 3.1).

If hydrogen or oxygen is differentially affected by reactions occurring at high temperatures in the TGA furnace such as oxide formation with the tin capsule material, or by H- or O-exchange reactions in the TGA furnace, the ratio of the measured δ^2H to $\delta^{18}O$ values should also change, reflecting the sequestration of oxygen into formation of oxide material. To assess any change in the ratio of measured δ values, we use the deuterium excess parameter of Dansgaard (1964), calculated as $d\text{-}excess = \delta^2H - 8 \times \delta^{18}O$, to evaluate the degree to which a

pair of measured δ^2H and $\delta^{18}O$ values deviates from the 8:1 relationship predicted by equilibrium fractionation, and observed in meteoric waters worldwide (Craig, 1961, Rozanski et al., 1993). Importantly, we are not using *d-excess* to infer any specific fractionation mechanism because the specific value of *d-excess* depends on the sample water and the calibration of δ^2H and $\delta^{18}O$ values (we present factory-calibrated data here). Since we are using factory calibrated δ^2H and $\delta^{18}O$ values to calculate and compare *d-excess* values, we only use it as a convenient and familiar metric to assess *relative* changes in δ^2H and $\delta^{18}O$ values from sample to sample. If different analysis temperatures were affecting δ^2H and $\delta^{18}O$ values differently, *d-excess* values would reflect this.

Figure 3C shows *d-excess* values as a function of heating temperature for liquid water samples in tin capsules, and there is no relationship between *d-excess* and temperature ($R^2 <$ 0.2 in Fig. 3C). The increase in the range of *d-excess* values at higher temperatures is due to a decrease in analytical precision for both δ^2H and $\delta^{18}O$ values at higher temperatures, as discussed earlier. The lack of systematic bias in δ^2H, $\delta^{18}O$ and *d-excess* values with heating temperature suggests that there are not temperature-dependent H- or O-exchange reactions with the tin capsule material or in the TGA furnace, and we determine tin capsules to be a suitable material to encapsulate liquid water samples during TGA-IRIS analysis.

3.3 Sample size effect

The sensitivity of the TGA-IRIS technique to sample size was evaluated by measuring 81 samples of different amounts (331 nL to 1160 nL) of liquid water (CHC, GTW, NVW) in tin capsules at 150 °C or 300 °C heating temperature. The results using factory calibrated data (to avoid any bias introduced by calibration correction) are shown in Figure 4 as the offset in measured δ values from the known δ values (calculated as $\Delta\delta = \delta_{measured} - \delta_{true}$) to allow comparison between waters with differing hydrogen and oxygen isotopic composition. For hydrogen, there is no systematic relationship between measured δ^2H values and sample amount for samples heated at 150 °C ($R^2 = 0$, n = 31, $p = 0.36$) or 300 °C ($R^2 = 0$, n = 50, $p = 0.68$) (Fig. 4A). For O, there is a weak correlation between measured $\delta^{18}O$ values and sample amount

for samples heated at both 150 °C (R^2 = 0.36, n = 31, $p < 0.001$) and 300 °C (R^2 = 0.43, n = 50, $p < 0.001$) (Fig. 4B).

The lack of a sample size effect for δ^2H values suggests that no correction is needed when applying calibration relationships to measured δ^2H values. The similar slopes of the weak sample size effect that *may* be present for $\delta^{18}O$ values at 150 °C (-0.0023 ‰ nL^{-1}) and at 300 °C (-0.0021 ‰ nL^{-1}) suggests that the effect may be intrinsic to the TGA-IRIS method at other temperatures. However, the weak correlation between measured $\delta^{18}O$ values and sample size may be due to the small volumes of water resulting from TGA analysis. In a study utilizing induction heating sample introduction, sample size effects large enough to necessitate correction were not found until sample size was 3000 nL or greater (Cui et al., 2017). In addition, any size effect correction may be obviated if the range in size of the unknown samples (in H_2O mass or volume) is relatively small, and if calibration standards can be size matched to the unknowns. Based on these results that do not show a significant size effect, we do not apply a size correction to the results from this study. However, we recommend that sample size effects be evaluated in any study using TGA-IRIS.

3.4 Memory effect

The so-called Memory Effect refers to the hydrogen and oxygen stable isotope compositions of preceding samples having an influence on the results of a water sample (Olsen et al., 2006; Gupta et al., 2009; Munksgaard et al., 2014; Cui et al., 2017). To assess the memory effect in TGA-IRIS, consecutive analyses of sets of samples of each water standard with contrasting δ^2H and $\delta^{18}O$ values (CHC, GTW, and NVW) were made at 150 °C (n = 6 per set) and 300 °C (n = 5 per set). The Memory Coefficient (*M*) was used to quantify the carry-over from sample to sample (Van Geldern and Barth, 2012; Uemura et al., 2016), calculated as: *M* (%) = $(\delta_{CM} - \delta_{CT})/(\delta_{PT} - \delta_{CT}) \times 100$, where δ_{CM} is the current isotopic measurement, δ_{CT} is the true isotopic value of the current sample, δ_{PT} is the true isotopic value of the previous water sample. To avoid introduced uncertainty from any calibration correction, factory calibrated measured values are used, and δ_{CT} and δ_{PT} are calculated as the average of the last three measurements of a sample set.

Memory coefficient (*M*) results at 150 °C and 300 °C are shown in Figure 5 (data in Supp. Table 2). If there was a memory effect present in this set of analyses from sets of water samples with progressively higher δ values, *M* values would be consistently negative in sign due to the influence of preceding samples with lower δ values. *M* values in Fig. 5 do not show such an influence in the initial analysis that follow a change in δ values that would indicate influence from previous analyses. *M* values in Fig. 5 are also generally similar to the range of *M* values that would be indistinguishable from analytical precision (grey bars in Fig. 5). We interpret the lack of M value trends, and the similarity between the magnitude of observed M values to that expected from analytical uncertainty at both 150 °C and 300 °C heating temperature to indicate that there is little or no sample memory effect for the TGA-IRIS system.

The lack of memory effect for TGA-IRIS contrasts with studies that found memory effects in both liquid water samples (Gupta et al., 2009; Munksgaard et al., 2014; Uemura et al 2016), and induction heating IRIS on waters bound into solid matrices (Cui et al., 2017). We attribute the lack of memory in TGA-IRIS to several aspects intrinsic to the technique itself. First, the water volumes measured in the TGA-IRIS technique are very small (typically < 1000 nL). Secondly, the high temperatures in the TGA furnace are higher than the vaporization point

of H_2O and isothermal times of 10 minutes at these elevated temperatures effectively "bake out" water that adsorbs to the internal system surfaces. Thirdly, all parts of the TGA-IRIS system in contact with water vapor are maintained at ≥80 °C thus preventing water adsorption and condensation. Finally, the TGA furnace flushes after every sample during cool down for > 10 minutes, while N_2 carrier gas flow rates remain at 25 mL min^{-1} thus maintaining dry internal TGA-IRIS system surfaces. At every step of the analysis, ≥ 5 min of N_2 carrier gas flushes residual water from the system between water vapor pulses (the flush time depends on the heating scheme and isothermal durations).

3.6 TGA-IRIS analyses of mineral hydration waters

In the following, we describe activities to demonstrate and validate measurements of δ^2H and $\delta^{18}O$ values by TGA-IRIS on hydration waters in synthetic and natural goethite samples. The choice of goethite to demonstrate the potential novel applications of TGA-IRIS was made due to goethite's widespread occurrence at Earth's surface and in the geologic rock record, and the well-established use of their isotopic compositions as records of paleoclimate conditions (e.g. Savin and Epstein, 1970; Yapp and Pedley, 1985; Yapp, 1987; Shepard and Gilg, 1996; Savin and Hsieh, 1998; Girard et al., 2000; Yapp, 2001; Feng and Yapp 2009; Yapp and Shuster, 2011).

3.6.1 TGA-IRIS analysis of goethite hydration waters

Heating of goethite yields H_2O by dehydration and dehydroxylation as illustrated by the schematic dehydroxylation reaction as it transforms to hematite (Deer et al., 1962; Boily et al., 2006):

$$2FeO(OH) \rightarrow Fe_2O_3 + H_2O \quad (1)$$

The thermal conversion of goethite to hematite is thought to be a solid-state topotactic reaction that occurs as a reaction front starting at grain boundaries which migrate into the

interior of grains, developing a transition state volume that moves with the reaction front as the reaction proceeds through the mineral grain (Hancock and Sharp, 1972; Goss, 1987; Yapp, 2003). As the reaction front progresses, microfractures develop in the product hematite, through which H_2O vapor escapes (Goss, 1987; Yapp, 2003).

To assess the H_2O release curves and determine the appropriate flash-heating temperatures for subsequent IRIS isotope analysis for goethites, we heated samples of SynGoethite2 and FCol-3 in the TGA at 10 °C min^{-1}, which allows the analyst to determine the specific temperature(s) at which mass loss occurs for each material, and therefore define the appropriate flash-heating scheme for each material. The slow heating scheme yielded mass loss from SynGoethite2 (starting sample mass of 8.116 mg) between 35 °C and 105 °C of 0.133 mg; (1.6%); and between 105 °C and 280 °C of 0.855 mg (10.5%) (Fig. 6). We note that for SynGoethite2, the slow heating resulted in a continuum of mass loss up to ~150 °C, and the water available at those temperatures was not fully released because not enough time was spent in this temperature range. This is a good illustration of the need to define both the temperature of each step for subsequent isotope analysis, as well as the isothermal duration of each temperature step to ensure complete water yield at that temperature. If there is incomplete water recovery at a temperature step, the isotope values of the water yielded at the subsequent temperature step will be biased by mixing. Slow heating of FCol-3 (starting sample mass of 6.519 mg) yielded mass loss between 250 °C and 370 °C of 0.59 mg (9.1%) (Fig. 6), and mass between 370 and 600 °C of 0.044 mg (0.8%), the total of which is 9.9%. This mass loss is the same (within analytical uncertainty) as the 9.8% ($\pm$ 0.2%) H_2O yielded by thermal decomposition for IRMS analyses for δ^2H values of FCol-3 material (Yapp and Poths, 1995). H_2O yields from both goethites were close to that predicted (10.14%) to be yielded from removal of OH^- species from stoichiometric goethite by thermal conversion to hematite (Eqn 1). Deviations in water yield may be due to a small amount of impurities in each sample, or non-stoichiometric mineral composition.

Mass lost at the 35 to 105 °C interval represents dehydration of weakly-adsorbed water on goethite mineral surfaces (Ford and Bertsch, 1999), and represents the atmospheric moisture the sample has most recently been exposed to. Mass lost between 105 °C and 280 °C

or 380 °C (SynGoethite2 and FCol-3, respectively) results from progressive dehydroxylation of OH^- from singly- through triply-coordinated hydroxo groups in the transition volume as goethite transforms to hematite (Boily et al., 2006; Song and Boily, 2016). The specific temperature at which the goethite to hematite transition occurs is primarily related to mineral crystallinity (e.g. Schwertmann, 1984; Ford and Bertsch, 1999; Song and Boily, 2016). The H_2O release from SynGoethite2 at 280 °C is likely due to low crystallinity corresponding to laboratory synthesis, whereas FCol-3 is a well-crystallized natural goethite (Yapp and Pedley, 1985; Yapp and Poths, 1995), resulting in higher H_2O release temperatures.

Based on the H_2O mass loss-temperature curve of SynGoethite2 (Fig. 6), we flash heated size-matched samples of SynGoethite2 (n = 5, average starting mass of 6.05 mg (± 0.69 mg)) to 105 °C and then to 280 °C (in separate successive steps) to rapidly release all of the water in each "pool" as a single pulse of sufficient peak size for reliable IRIS analysis. For FCol-3, we used larger samples (n = 4, average starting mass of 19.00 mg (± 2.36 mg)) because of lower H_2O yields than SynGoethite2 (Fig. 6), and flash-heated the samples to 105 °C and 370 °C. Heating beyond the major water-yielding points of 280 °C and 370 °C up to 600 °C did not release sufficient H_2O from either goethite to generate a sample peak large enough to reliably analyze.

The reproducibility (± 1 S.D.) of TGA-IRIS measurements on SynGoethite2 was 1.63‰ for δ^2H and 0.27‰ for $\delta^{18}O$ values at 105 °C, and was 1.21‰ for δ^2H and 0.17‰ for $\delta^{18}O$ values at 280 °C, and we therefore interpret these as the precision of δ values for water released from SynGoethite2 at 105 °C and 280 °C. These analytical precisions are similar or better than that of liquid water samples at 150 °C ($\delta^2H \pm 1.23$‰, $\delta^{18}O \pm 0.17$‰) and 300 °C ($\delta^2H \pm 0.68$‰, $\delta^{18}O \pm 0.52$‰, see Section 3.2), which suggests that the use of liquid water as calibration standards is sufficient to conservatively estimate precision of mineral hydration water analyses. However, it also suggests that if mineral standards can be prepared or obtained that are sufficiently isotopically homogeneous, and used for calibration during analytical runs, that precision estimates and calibrations for water released by solid samples can be further constrained. All of the δ^2H and $\delta^{18}O$ values presented here for goethite materials were calibrated using liquid water standards included during each analytical run (Table 1).

3.6.2 δ^2H values of goethite hydration waters by TGA-IRIS

Except for the H_2O weakly adsorbed to mineral surfaces, hydrogen is present in goethite only in the OH^- that is bonded in Fe-O groups (Ford and Bertsch, 1999; Cornell and Schwertmann, 2003; Boily et al., 2006; Song and Boily, 2016). Measurements of the hydrogen isotopic composition of goethite by TGA-IRIS and IRMS should be comparable as the H-bearing reservoir in goethite is accessible to both methods via thermal dehydroxylation.

Analysis of SynGoethite2 by TGA-IRIS (n = 5) at 280 °C (after initial heating to 105 °C to remove adsorbed water) gives an average δ^2H value of -158.2‰ (± 1.2‰) (Table 2). The mineral-water fractionation factor for hydrogen ($\propto^H_{m-w}$) calculated from the average δ^2H value by TGA-IRIS analysis of SynGoethite2 and the δ^2H value of the water used to synthesize the material at 22 C is 0.906. This value of $\propto^H_{m-w}$ is the same, within analytical uncertainty, as the generally accepted literature $\propto^H_{m-w}$ value of 0.905 (Yapp, 1987; Yapp, 2001).

Analysis of FCol-3_Goet by TGA-IRIS (n = 4) at 370 °C results in an average δ^2H value of -138.2‰ (± 0.3‰) (Fig. 7), which is similar to that of -131‰ (± 2‰) measured by IRMS on FCol-3 material (Table 2) (Yapp and Poths, 1995). The mineral-water fractionation factor for hydrogen ($\propto^H_{m-w}$) calculated from the average δ^2H value by TGA-IRIS analysis of FCol-3 and the δ^2H value (-110‰) of the water postulated to have been the source water during goethite formation at the same locality as FCol-3 (FCol-1 in Yapp and Pedley, 1985) is 0.968. This value of $\propto^H_{m-w}$ is similar to that calculated for FCol-1 ($\propto^H_{m-w} = 0.971$) by Yapp and Pedley (1985), which is expected from the similarity in measured goethite δ^2H values by the two methods and the same postulated source water value. However, these $\propto^H_{m-w}$ values from FCol goethite differ from the literature $\propto^H_{m-w}$ value 0.905 ± 0.004 (Yapp, 1987; Yapp, 2001). Yapp and Pedley (1985) note that FCol goethite has the highest $\propto^H_{m-w}$values of the 21 natural goethites they analyzed, though neither our analyses or theirs are able to resolve the reasons for this disparity.

Based on the similarity of H_2O yields during TGA-IRIS analyses to that predicted by stoichiometry, as well as the similarity of mineral-water fractionation factors for hydrogen ($\propto^H_{m-w}$) derived from both TGA-IRIS and IRMS on a synthetic and a natural goethite material, we conclude that that TGA-IRIS analyses of hydrogen isotopes in goethite produces δ^2H values

that reflect the total hydrogen of the goethite. TGA-IRIS δ^2H values from goethite should be comparable to those made by IRMS and found in the literature.

3.6.3 $\delta^{18}O$ values of goethite hydration waters by TGA-IRIS

Oxygen is present in goethite in two bonded groups: Fe-O and Fe-OH^- (Ford and Bertsch, 1999; Cornell and Schwertmann, 2003; Boily et al., 2006; Song and Boily, 2016). The oxygen in the water evolved by thermal dehydroxylation of goethite and its transition to hematite during TGA-IRIS analysis (and resulting $\delta^{18}O_{OH}$ values) is only 50% of the oxygen in the Fe-OH^- groups, while the remaining 50% is incorporated into the resulting hematite (Eqn. 1). In contrast, oxygen recovered from goethite by fluorination and IRMS analysis will be all of the O in goethite, from both Fe-O and Fe-OH^- groups ($\delta^{18}O_{Total}$). Thus, values of $\delta^{18}O_{OH}$ made by TGA-IRIS on goethite should not be not directly comparable to $\delta^{18}O_{Total}$ measurements made by fluorination and IRMS.

The absence of oxygen isotope exchange between the Fe-O and Fe-OH groups as goethite undergoes the topotactic transformation to hematite, as represented by Eqn 1, underpins the interpretation of $\delta^{18}O_{OH}$ values yielded by TGA-IRIS analysis. Previous work shows that neither goethite nor hematite readily exchange structural oxygen isotopes with water (Becker and Clayton, 1976; Yapp, 1991). In a study comparing open- and closed-system thermal dehydration of goethite conversion to hematite, Yapp (1990) showed that in open-systems under vacuum, minimal reversible mineral-vapor oxygen isotope exchange was likely, though its complete absence was not demonstrated conclusively. The TGA-IRIS system is open as the released H_2O vapor is continually removed by N_2 carrier gas, and as such it is likely that back-exchange of oxygen either does not occur in the H_2O vapor-mineral system, or that it is minimal. The short timescales of H_2O vapor release during TGA flash heating during TGA-IRIS analysis (thermal conversion complete within < 300 seconds) also does not favor solid-state oxygen diffusion and exchange.

Analysis of SynGoethite2 by TGA-IRIS (n = 5) at 280 °C (after initial heating to 105 °C to remove adsorbed water) gives an average $\delta^{18}O_{OH}$ value of -10.64‰ (± 0.17‰) (Table 2). The

mineral-water fractionation factor for oxygen in SynGoethite2 between O_{OH} and the source water ($\propto_{m-w}^{O,OH}$) calculated from the average $\delta^{18}O_{OH}$ value by TGA-IRIS analysis of SynGoethite2 and the $\delta^{18}O_{H2O}$ value of the water used to synthesize the material at 22 °C is $\propto_{m-w}^{O,OH}$ = 0.9972 (Table 2). As noted, goethite oxygen mineral-hydration water fractionation factors ($\propto_{m-w}^{O,OH}$ values) derived from TGA-IRIS analyses are not directly comparable to total oxygen mineral-water fractionation factors ($\propto_{m-w}^{O,Total}$ values) because each oxygen reservoir in the original goethite may differ in isotopic composition, and a comparison between the two fractionation factors may indicate whether the two oxygen reservoirs do differ isotopically. Indeed, the SynGoet2 $\propto_{m-w}^{O,OH}$ value of 0.9972 is significantly different than literature $\propto_{m-w}^{O,Total}$ values of 0.985 for goethite synthesized at 22 °C and at high pH by Bao and Koch (1999) (conditions which match that used to synthesize SynGoet2). This difference in $\propto_{m-w}^{O,OH}$ and $\propto_{m-w}^{O,Total}$ values for goethite suggests that the oxygen in the Fe-OH and Fe-O bound groups do not have the same isotopic composition, and thus an internal oxygen isotope fractionation relationship may exist for goethite.

Analysis of FCol-3 by TGA-IRIS (n = 4) at 370 °C (after initial heating to 105 °C) gives an average $\delta^{18}O_{OH}$ value of -4.72‰ (± 0.32‰) (Fig. 7, Table 2). For FCol-3, the value of $\propto_{m-w}^{O,OH}$ = 1.0103, using TGA-IRIS measurements of $\delta^{18}O_{OH}$ values and $\delta^{18}O_{H2O}$ values of the postulated source water for FCol-3 (Yapp and Pedley, 1985; Yapp, 1987). We are not able to rigorously compare FCol-3 $\propto_{m-w}^{O,OH}$ values to $\propto_{m-w}^{O,Total}$ values because the source water for FCol-3 formation is not exactly known, and instead is postulated based on measured $\delta^{2}H_{Total}$ values (Yapp and Pedley, 1985, Yapp, 1987) combined with the modern globally averaged relationship of $\delta^{2}H$ to $\delta^{18}O$ in precipitation (Rozanski, et al., 1993). However, a tentative comparison between FCol-3 $\propto_{m-w}^{O,OH}$ = 1.0103 and $\propto_{m-w}^{O,Total}$ = 1.0168, again reveals possible differences in the oxygen isotope composition of the Fe-OH and Fe-O groups.

Complicating interpretations and comparison of the oxygen isotope composition of the Fe-OH and Fe-O groups in goethite, is the recovery of only 50% of the $Fe\text{-}OH^{-}$ oxygen by TGA-IRIS, as the remaining 50% is incorporated into the residual hematite. Whether the residual hematite oxygen preserves the initial goethite $Fe\text{-}OH^{-}$ $\delta^{18}O_{OH}$ values, or if it is affected by a possible kinetic fraction as water vapor is evolved under open system conditions, as suggested

by Yapp (2003), remains to be investigated further. The relationship between the goethite $\propto_{m-w}^{O,OH}$ values determined by TGA-IRIS and the factors of source water and mineral formation temperature are not interpretable without further studies to constrain how goethite $\propto_{m-w}^{O,OH}$ values vary with these factors, as has been done for goethite $\propto_{m-w}^{O,Total}$ values (e.g. Yapp, 2001). We are also not able to determine why the $\propto_{m-w}^{O,OH}$ value for SynGoethite2 is < 1, and $\propto_{m-w}^{O,OH}$ value for FCol-3 is > 1, but it may be related to the pH of mineral formation, the degree of crystallinity for each material, as well as the presence of high-temperature nonstoichiometric water in SynGoethite2. However, the indication that an oxygen isotope distinction exists for Fe-OH and Fe-O in goethite adds to the evidence of the possibility that goethite can serve as a single-mineral geothermometer (Yapp, 1987). Further research is needed to confirm these initial results, and to further evaluate the meaning of the $\delta^{18}O$ values of the water derived from goethite during TGA-IRIS analysis.

3.7 Appraisal of the TGA-IRIS method

The TGA-IRIS method presents some advantages over currently available techniques to liberate water from solid samples for hydrogen and oxygen stable isotope analysis. The range of temperature and heating duration available allows TGA-IRIS to be applied more flexibly than methods using a single temperature (often very high) and single duration such as by microwave or induction heating. Quantifying mass loss at specific temperatures in succession is also useful information itself, which is not readily available by other methods. TGA-IRIS is likely to be applicable to nearly any hydrated material, including hydrous minerals such as clays, or hydrated glass. Because hydrated minerals have specific temperatures of water yield, it may be possible to analyze mineral-specific hydration waters in multi-mineral materials (such as soils) in the same sample aliquot. It seems possible to miniaturize TGA-IRIS systems for transport to remote locations, and the presence of goethite and hydrated Fe oxide minerals on the surface of Mars, presents the opportunity for possible future application of TGA-IRIS to extraplanetary settings.

TGA-IRIS is not without its limitations, some of which may be resolvable with continued development. The cost of the TGA instrument is significant, especially compared to microwave

heating equipment. Only small samples (~ <100 mg) can be analyzed, depending on the TGA instrument, which may be a limitation in heterogeneous materials. Samples with high humidity or moisture content may present difficulties for sample handling to avoid pre-analysis evaporation or reduced precision due to incomplete TGA furnace pre-flushing (see discussion regarding liquid water samples). Any pre-evaporation effect will be largest in small samples.

4. Conclusions

We have presented an approach for the stable isotope analysis of liquid and mineral-hydration waters based on coupling of thermogravimetric analysis with isotope ratio infrared spectroscopy (TGA-IRIS). TGA-IRIS presents an approach to the analysis of mineral hydration waters that is versatile and requires almost no preparation of mineral samples, other than to clean them. TGA-IRIS analyses of hydrogen stable isotopes in goethite hydration water yields δ^2H values that reflect the hydrogen of the OH^- phase in the mineral and are comparable to that made by IRMS and found in the literature. In contrast, $\delta^{18}O$ values reflect the oxygen in the Fe-OH bonded group, and not the oxygen bound in the Fe-O group in the mineral crystal lattice. Therefore, $\delta^{18}O$ values of goethite hydration water by TGA-IRIS are not directly comparable to literature $\delta^{18}O$ values that reflect the total O. However, because TGA-IRIS can yield only the Fe-OH bonded oxygen, it may be possible to combine these results with measurements of the Fe-O bonded oxygen in the resulting hematite by fluorination and IRMS to determine if the fractionation factors for oxygen in the Fe-OH and Fe-O groups differ.

The ability of TGA-IRIS to generate detailed mineral hydration water yield data and δ^2H and $\delta^{18}O$ values of yielded water at varying temperatures, allows for the differentiation of water in varying states of binding on and within the mineral matrix. TGA-IRIS analysis also yields δ^2H and $\delta^{18}O$ values on the same sample, which presents advantages in materials with limited sample size or availability. In addition, the ease with which TGA-IRIS measurements of hydration waters can be made opens new avenues and possibilities for research on hydrated minerals.

599
600 **Acknowledgements**
601
602 This work was performed under the auspices of the U.S. Department of Energy by
603 Lawrence Livermore National Laboratory under Contract DE-AC52-07NA27344. This submission
604 is LLNL-JRNL-736485. The constructive reviews of Crayton Yapp and an anonymous reviewer
605 improved this paper.
606
607
608 **References**
609
610 Araguas-Araguas, L., Rozanski, K., Gonfiantini, R. and Louvat, D. (1995) Isotope effects
611 accompanying vacuum extraction of soil water for stable isotope analyses. Journal of Hydrology
612 168, 159-171.
613
614 Bao, H. and Koch, P.L. (1999) Oxygen isotope fractionation in ferric oxide-water systems: low
615 temperature synthesis. Geochimica et Cosmochimica Acta 63, 599-613.
616 Becker, R.H. and Clayton, R.N. (1976) Oxygen isotope study of a Precambrian banded iron-
617 formation, Hamersley Range, Western Australia. Geochimica et Cosmochimica Acta 40, 1153-
618 1165.
619
620 Boily, J.-F., Szanyi, J. and Felmy, A.R. (2006) A combined FTIR and TPD study on the bulk and
621 surface dehydroxylation and decarbonation of synthetic goethite. Geochimica et Cosmochimica
622 Acta 70, 3613-3624.
623
624 Bowen, G.J. (2010) Isoscapes: spatial pattern in isotopic biogeochemistry. Annual Review of
625 Earth and Planetary Sciences 38, 161-187.
626 Clayton, R.N. and Mayeda, T.K. (1963) The use of bromine pentafluoride in the extraction of
627 oxygen from oxides and silicates for isotopic analysis. Geochimica et cosmochimica acta 27, 43-
628 52.

Coplen, T.B. (1994) Reporting of stable hydrogen, carbon, and oxygen isotopic abundances (technical report). Pure and Applied Chemistry 66, 273-276.

Cornell, R.M. and Schwertmann, U. (2003) The iron oxides: structure, properties, reactions, occurrences and uses. John Wiley & Sons.

Craig, H. (1961) Isotopic variations in meteoric waters. Science 133, 1702-1703.

Cui, J., Tian, L., Gerlein-Safdi, C. and Qu, D. (2017) The influence of memory, sample size effects, and filter paper material on online laser-based plant and soil water isotope measurements. Rapid Communications in Mass Spectrometry 31(6), 509-522.

Dansgaard, W. (1964) Stable Isotopes in Precipitation. Tellus 16, 436-468.

Deer, W.A., Howie, R.A. and Zussman, J. (1962) An introduction to the rock-forming minerals.

Deer, W.A., Howie, R.A., Zussman, J. and Deer, W.A. (1963) Rock-forming minerals. 3 (1963). Sheet silicates. Longmans.

Feng, W. and Yapp, C.J. (2009) 18 O/16 oxygen and D/H ratios of pedogenic kaolinite in a North American Cenomanian laterite: Paleoclimatic implications. Geochimica et Cosmochimica Acta 73, 6249-6263.

Ford, R.G. and Bertsch, P.M. (1999) Distinguishing between surface and bulk dehydration-dehydroxylation reactions in synthetic goethites by high-resolution thermogravimetric analysis. Clays and Clay Minerals 47, 329-337.

657 Friedman, I. and O'Neil, J.R. (1977) Compilation of stable isotope fractionation factors of
658 geochemical interest. Professional Paper 440-KK, United States Geological Survey, Washington
659 D.C.
660
661 Garrels, R.M. and Christ, C.L. (1965) Solutions, minerals, and equilibria. Harper and Row, New
662 York, 450 p.
663
664 Geldern, R. and Barth, J.A. (2012) Optimization of instrument setup and post-run corrections for
665 oxygen and hydrogen stable isotope measurements of water by isotope ratio infrared
666 spectroscopy (IRIS). Limnology and Oceanography: Methods 10, 1024-1036.
667
668 Girard, J.-P., Freyssinet, P. and Chazot, G. (2000) Unraveling climatic changes from intraprofile
669 variation in oxygen and hydrogen isotopic composition of goethite and kaolinite in laterites: an
670 integrated study from Yaou, French Guiana. Geochimica et Cosmochimica Acta 64, 409-426.
671
672 Goss, C. (1987) The kinetics and reaction mechanism of the goethite to hematite
673 transformation. Mineralogical Magazine 51, 437-451.
674
675 Gupta, P., Noone, D., Galewsky, J., Sweeney, C. and Vaughn, B.H. (2009) Demonstration of high-
676 precision continuous measurements of water vapor isotopologues in laboratory and remote
677 field deployments using wavelength-scanned cavity ring-down spectroscopy (WS-CRDS)
678 technology. Rapid communications in mass spectrometry 23, 2534-2542.
679
680 Hamza, M. and Epstein, S. (1980) Oxygen isotopic fractionation between oxygen of different
681 sites in hydroxyl-bearing silicate minerals. Geochimica et Cosmochimica Acta 44, 173-182.
682
683 Hancock, J. and Sharp, J. (1972) Method of Comparing Solid-State Kinetic Data and Its
684 Application to the Decomposition of Kaolinite, Brucite, and BaCO3. Journal of the American
685 Ceramic Society 55, 74-77.

Hendry, M., Schmeling, E., Wassenaar, L., Barbour, S. and Pratt, D. (2015) Determining the stable isotope composition of pore water from saturated and unsaturated zone core: improvements to the direct vapour equilibration laser spectrometry method. Hydrology and Earth System Sciences 19, 4427.

Johnson, J., Hamann, L., Dettman, D., Kim-Hak, D., Leavitt, S., Monson, R. and Papuga, S. (2016) Performance of induction module-cavity ring-down spectroscopy (IM-CRDS) for measuring δ18O and δ2H values of soil, stem, and leaf waters. Rapid Communications in Mass Spectrometry 31(6), 547-560.

Kerr, P.F. (1950) Analytical data on reference clay materials. No. 7, Columbia University, New York.

Kerstel, E. and Gianfrani, L. (2008) Advances in laser-based isotope ratio measurements: selected applications. Applied Physics B: Lasers and Optics 92, 439-449.

Kerstel, E.T., Van Trigt, R., Reuss, J. and Meijer, H. (1999) Simultaneous determination of the 2H/1H, 17O/16O, and 18O/16O isotope abundance ratios in water by means of laser spectrometry. Analytical Chemistry 71, 5297-5303.

Koehler, G., Wassenaar, L.I., (2012) Determination of the hydrogen isotopic compositions of organic materials and hydrous minerals using thermal combustion – OA-ICOS laser spectroscopy. Analytical Chemistry 84, 3640-3645.

Koehler, G., Wassenaar, L.I. and Hendry, J. (2013) Measurement of stable isotope activities in saline aqueous solutions using optical spectroscopy methods. Isotopes in environmental and health studies 49, 378-386.

714 Lawrence, J.R. and Taylor, H.P. (1971) Deuterium and oxygen-18 correlation: Clay minerals and
715 hydroxides in Quaternary soils compared to meteoric waters. Geochimica et Cosmochimica
716 Acta 35, 993-1003.

717 Lawrence, J. and Taylor, H. (1972) Hydrogen and oxygen isotope systematics in weathering
718 profiles. Geochimica et Cosmochimica Acta 36, 1377-1393.

719 Maher, K. and Chamberlain, C. (2014) Hydrologic regulation of chemical weathering and the
720 geologic carbon cycle. Science 343, 1502-1504.
721
722 Munksgaard, N.C., Cheesman, A.W., Wurster, C.M., Cernusak, L.A. and Bird, M.I. (2014)
723 Microwave extraction–isotope ratio infrared spectroscopy (ME-IRIS): a novel technique for
724 rapid extraction and in-line analysis of δ18O and δ2H values of water in plants, soils and insects.
725 Rapid Communications in Mass Spectrometry 28, 2151-2161.
726
727 Munksgaard, N.C., Wurster, C.M. and Bird, M.I. (2011) Continuous analysis of δ18O and δD
728 values of water by diffusion sampling cavity ring-down spectrometry: a novel sampling device
729 for unattended field monitoring of precipitation, ground and surface waters. Rapid
730 Communications in Mass Spectrometry 25, 3706-3712.
731
732 Mustard, J.F., Murchie, S., Pelkey, S., Ehlmann, B., Milliken, R., Grant, J., Bibring, J.-P., Poulet, F.,
733 Bishop, J. and Dobrea, E.N. (2008) Hydrated silicate minerals on Mars observed by the Mars
734 Reconnaissance Orbiter CRISM instrument. Nature 454, 305-309.
735
736 Méheut, M., Lazzeri, M., Balan, E. and Mauri, F. (2007) Equilibrium isotopic fractionation in the
737 kaolinite, quartz, water system: Prediction from first-principles density-functional theory.
738 Geochimica et Cosmochimica Acta 71, 3170-3181.
739
740 Nesbitt, H. and Young, G.M. (1989) Formation and diagenesis of weathering profiles. The
741 Journal of Geology 97, 129-147.

Oerter, E.J., Perelet, A., Pardyjak, E. and Bowen, G. (2017a) Membrane inlet laser spectroscopy to measure H and O stable isotope compositions of soil and sediment pore water with high sample throughput. Rapid Communications in Mass Spectrometry 31, 75-84.

Oerter, E.J., Malone, M., Putnam, A., Drits-Esser, D., Stark, L. and Bowen, G. (2017b) Every apple has a voice: using stable isotopes to teach about food sourcing and the water cycle. Hydrology and Earth System Sciences 21, 3799-3810.

Oerter, E.J. and Bowen, G. (2017) In situ monitoring of hydrogen and oxygen stable isotopes in soil water reveals ecohydrologic dynamics in managed soil systems. Ecohydrology 10(4).

Olsen, J., Seierstad, I., Vinther, B., Johnsen, S. and Heinemeier, J. (2006) Memory effect in deuterium analysis by continuous flow isotope ratio measurement. International Journal of Mass Spectrometry 254, 44-52.

Orlowski, N., Pratt, D.L. and McDonnell, J.J. (2016) Intercomparison of soil pore water extraction methods for stable isotope analysis. Hydrological Processes 30, 3434-3449.

Rohrssen, M., Brunner, B., Mielke, R.E. and Coleman, M. (2008) Method for simultaneous oxygen and hydrogen isotope analysis of water of crystallization in hydrated minerals. Analytical chemistry 80, 7084-7089.

Rothfuss, Y., Vereecken, H. and Brüggemann, N. (2013) Monitoring water stable isotopic composition in soils using gas-permeable tubing and infrared laser absorption spectroscopy. Water Resources Research 49, 3747-3755.

Rozanski, K., Araguas-Araguas, L. and Giofiantini, R. (1993) Isotopic patterns in modern global precipitation. Geophysical Monograph 78, 1-36.

771

772 Savin, S.M. and Epstein, S. (1970) The oxygen and hydrogen isotope geochemistry of clay
773 minerals. Geochimica et Cosmochimica Acta 34, 25-42.
774
775 Savin, S.M. and Hsieh, J.C. (1998) The hydrogen and oxygen isotope geochemistry of pedogenic
776 clay minerals: principles and theoretical background. Geoderma 82, 227-253.
777
778 Schwertmann, U. (1984) The double dehydroxylation peak of goethite. Thermochimica Acta 78,
779 39-46.
780
781 Schwertmann, U., Cornell, R. M., (2003). The iron oxides: structure, properties, reactions,
782 occurrences and uses. John Wiley & Sons.
783
784 Sharp, Z., Atudorei, V. and Durakiewicz, T. (2001) A rapid method for determination of
785 hydrogen and oxygen isotope ratios from water and hydrous minerals. Chemical Geology 178,
786 197-210.
787
788 Sheppard, S. and Gilg, H. (1996) Stable isotope geochemistry of clay minerals. Clay Minerals 31,
789 1-24.
790
791 Singer, M.J. and Nkedi-Kizza, P. (1980) Properties and history of an exhumed Tertiary Oxisol in
792 California. Soil Science Society of America Journal 44, 587-590.
793
794 Song, X. and Boily, J.-F. (2016) Surface and Bulk Thermal Dehydroxylation of FeOOH
795 Polymorphs. The Journal of Physical Chemistry A 120, 6249-6257.
796
797 Uemura, R., Nakamoto, M., Asami, R., Mishima, S., Gibo, M., Masaka, K., Jin-Ping, C., Wu, C.-C.,

798 Chang, Y.-W. and Shen, C.-C. (2016) Precise oxygen and hydrogen isotope determination in
799 nanoliter quantities of speleothem inclusion water by cavity ring-down spectroscopic
800 techniques. Geochimica et Cosmochimica Acta 172, 159-176.
801
802 Volkmann, T. and Weiler, M. (2014) Continual in-situ monitoring of pore water stable isotopes
803 in the subsurface. Hydrology and Earth System Sciences 18, 1819-1833.
804
805 Wassenaar, L.I., Hendry, M.J., Chostner, V.L. and Lis, G.P. (2008) High Resolution Pore Water
806 delta(2)H and delta(18)O Measurements by H(2)O((liquid))-H(2)O((vapor)) Equilibration Laser
807 Spectroscopy. Environmental Science & Technology 42, 9262-9267.
808
809 West, A.G., Goldsmith, G.R., Brooks, P.D. and Dawson, T.E. (2010) Discrepancies between
810 isotope ratio infrared spectroscopy and isotope ratio mass spectrometry for the stable isotope
811 analysis of plant and soil waters. Rapid Communications in Mass Spectrometry 24, 1948-1954.
812
813 Yang, C., Yang, S. and Su, N. (2016) Stable hydrogen and oxygen isotopes in mineral-bound
814 water and the indication for chemical weathering intensity. Chemical Geology 441, 14-23.
815
816 Yapp, C. (2001) Rusty relics of Earth history: Iron (III) oxides, isotopes, and surficial
817 environments. Annual Review of Earth and Planetary Sciences 29, 165-199.
818
819 Yapp, C.J. (1987) Oxygen and hydrogen isotope variations among goethites (α-FeOOH) and the
820 determination of paleotemperatures. Geochimica et Cosmochimica Acta 51, 355-364.
821
822 Yapp, C.J. (1990a) Oxygen isotopes in iron (III) oxides: 1. Mineral-water fractionation factors.
823 Chemical Geology 85, 329-335.
824
825 Yapp, C.J. (1990b) Oxygen isotope effects associated with the solid-state α-FeOOH to α-Fe2O3
826 phase transformation. Geochimica et Cosmochimica Acta 54, 229-236.

827

828 Yapp, C.J. (1991) Oxygen isotopes in an oolitic ironstone and the determination of goethite
829 δ18O values by selective dissolution of impurities: the 5M NaOH method. Geochimica et
830 Cosmochimica Acta 55, 2627-2634.
831
832 Yapp, C.J. (2003) A model for 18 O/16 oxygen variations in CO 2 evolved from goethite during
833 the solid-state α-FeOOH to α-Fe 2 oxygen 3 phase transition. Geochimica et cosmochimica acta
834 67, 1991-2004.
835
836 Yapp, C.J. (2008) 18 O/16 oxygen and D/H in goethite from a North American Oxisol of the early
837 Eocene climatic optimum. Geochimica et Cosmochimica Acta 72, 5838-5851.
838
839 Yapp, C.J. (2015) 18 O/16 oxygen in CO 2 evolved from goethite during some unusually rapid
840 solid state α-FeOOH to α-Fe 2 oxygen 3 phase transitions: Test of an exchange model for
841 possible use in oxygen isotope analyses of goethite. Geochimica et Cosmochimica Acta 170, 1-
842 16.
843
844 Yapp, C.J. and Pedley, M.D. (1985) Stable hydrogen isotopes in iron oxides—II. DH variations
845 among natural goethites. Geochimica et Cosmochimica Acta 49, 487-495.
846
847 Yapp, C.J. and Shuster, D.L. (2011) Environmental memory and a possible seasonal bias in the
848 stable isotope composition of (U–Th)/He-dated goethite from the Canadian Arctic. Geochimica
849 et Cosmochimica Acta 75, 4194-4215.
850
851

852 FIGURE CAPTIONS

853

854 Figure 1. TGA-IRIS liquid water analysis time trace example. [H_2O], δ^2H and $\delta^{18}O$ values
855 collected at approximately 1 Hz frequency throughout the analysis. Black circles ([H_2O]), blue
856 triangles (δ^2H), and red squares ($\delta^{18}O$) denote interval of water sample peak and duration of
857 signal integration, beginning when [H_2O] values increase above background, ending at [H_2O] =
858 2000 ppmV. Factory-calibrated data are shown. For color symbols, readers are referred to the
859 online version of this paper.

860

861 Figure 2. Relationship between the integrated sum of water vapor for each sample received at
862 the IRIS instrument and the liquid volume of each water sample for samples loaded in tin
863 capsules and flash heated at 150, 300, 450, and 600 °C. Sample volume calculated from sample
864 mass measured in the TGA, using 1 mg = 1000 nL H_2O at 25 °C.

865

866 Figure 3. Relationship between heating temperature in TGA-IRIS and measured (A) δ^2H values,
867 (B) $\delta^{18}O$ values, and (C) deuterium excess (d-excess) values of CHC liquid water samples in tin
868 capsules (factory calibrated data).

869

870 Figure 4. Plots showing relationships between sample size and offset in measured (A) δ^2H
871 values and (B) $\delta^{18}O$ values of liquid water samples in tin capsules measured by TGA-IRIS at 150
872 °C and 300 °C heating temperature. Offset in measured δ values are shown as $\Delta\delta = \delta_{measured} -$
873 δ_{true} (calculated with factory calibrated data) to allow comparison between waters with
874 differing hydrogen and oxygen isotopic composition.

875

876 Figure 5. Memory coefficients (M values) for successive samples of liquid water at (A and B) at
877 150 °C, and (C and D) at 300 °C. Grey regions in the plots represent range of memory
878 indistinguishable from analytical precision. Analysis # refers to the number of analyses
879 following a change in sample sets with differing δ values. Sample set sequence was: NVW (δ^2H =
880 -119.4‰ and $\delta^{18}O$ = -15.11‰), followed by GTW (δ^2H = -70.1‰ and $\delta^{18}O$ = -9.40‰), followed
881 by CHC (δ^2H = -24.4‰ and $\delta^{18}O$ = -2.51‰).

Figure 6. Weight loss (%) during thermogravimetric analysis of SynGoet2 (medium-dash blue line) and FCol-3 (short-dash red line) samples in this study, and the derivative weight loss with respect to time (SynGoet2: solid blue line, FCol-3: dash-dot red line). Samples were heated at 10 °C min^{-1}. For color symbols, readers are referred to the online version of this paper.

Figure 7. TGA-IRIS analysis time trace of a FCol-3 goethite sample. [H_2O], δ^2H and $\delta^{18}O$ values collected at approximately 1 Hz frequency throughout the analysis. Black circles ([H_2O]), blue triangles (δ^2H), and red squares ($\delta^{18}O$) denote interval of water sample peak and duration of signal integration, beginning when [H_2O] values increase above background, ending at [H_2O] = 2000 ppmV. Factory-calibrated data are shown. For color symbols, readers are referred to the online version of this paper.

TABLE CAPTIONS

Table 1. δ^2H and $\delta^{18}O$ values of the water used as TGA-IRIS calibration standards

Table 2. Data for samples analyzed by TGA-IRIS in this study. Water yields, mineral hydration δ values, and mineral-hydration water fractionation factors in ($\propto_{m-w}^{O,OH}$) are averages of n analyses (± 1 standard deviation).

905 Figure 1

906

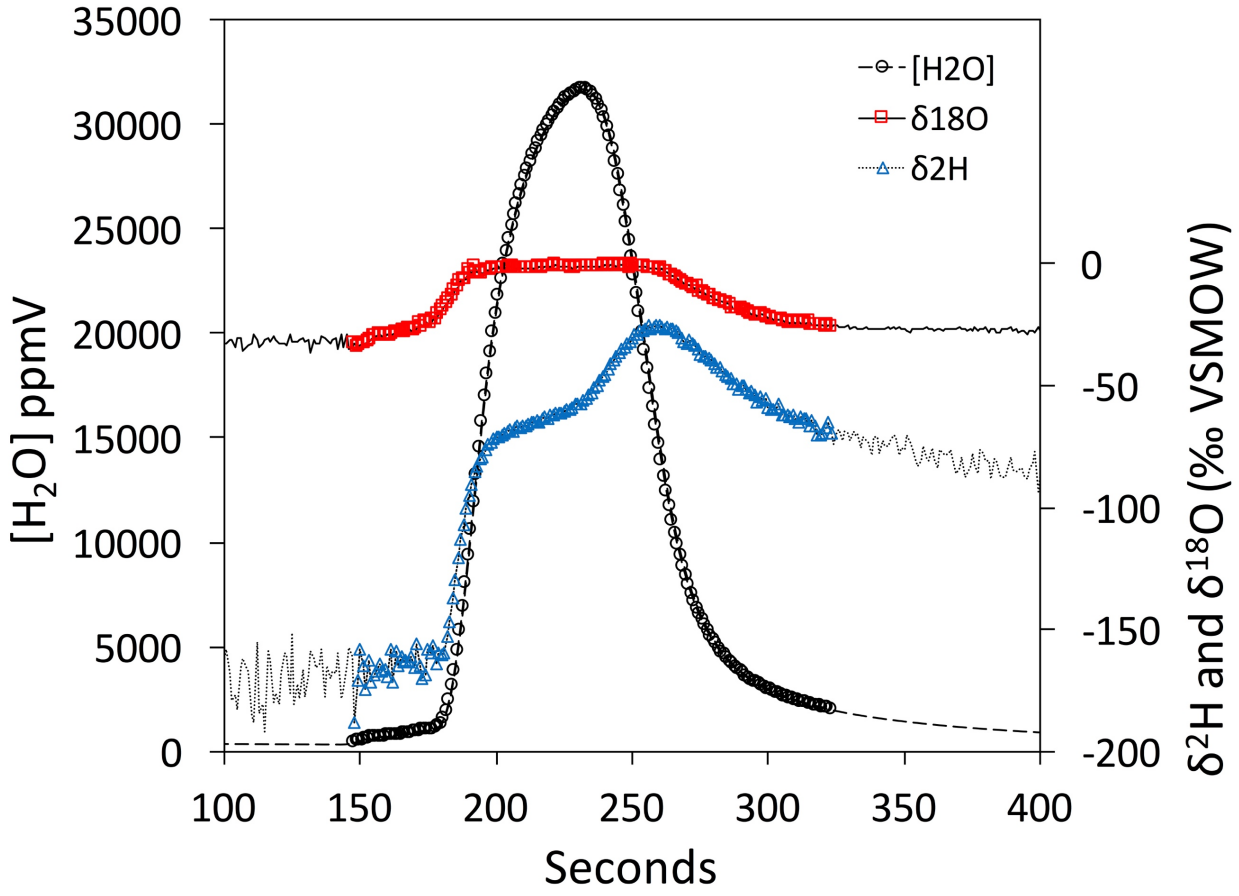

907

908

909

910 Figure 2

911

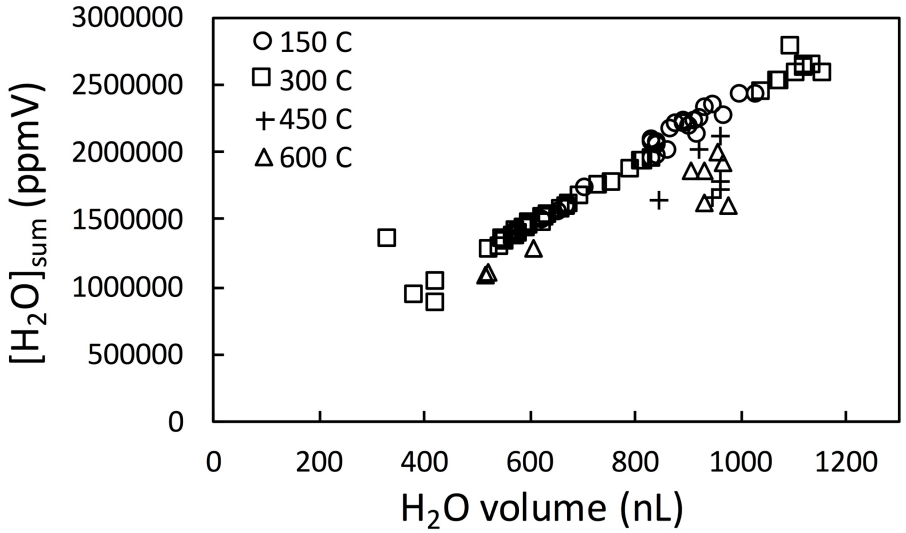

912

913

914

915 Figure 3

916

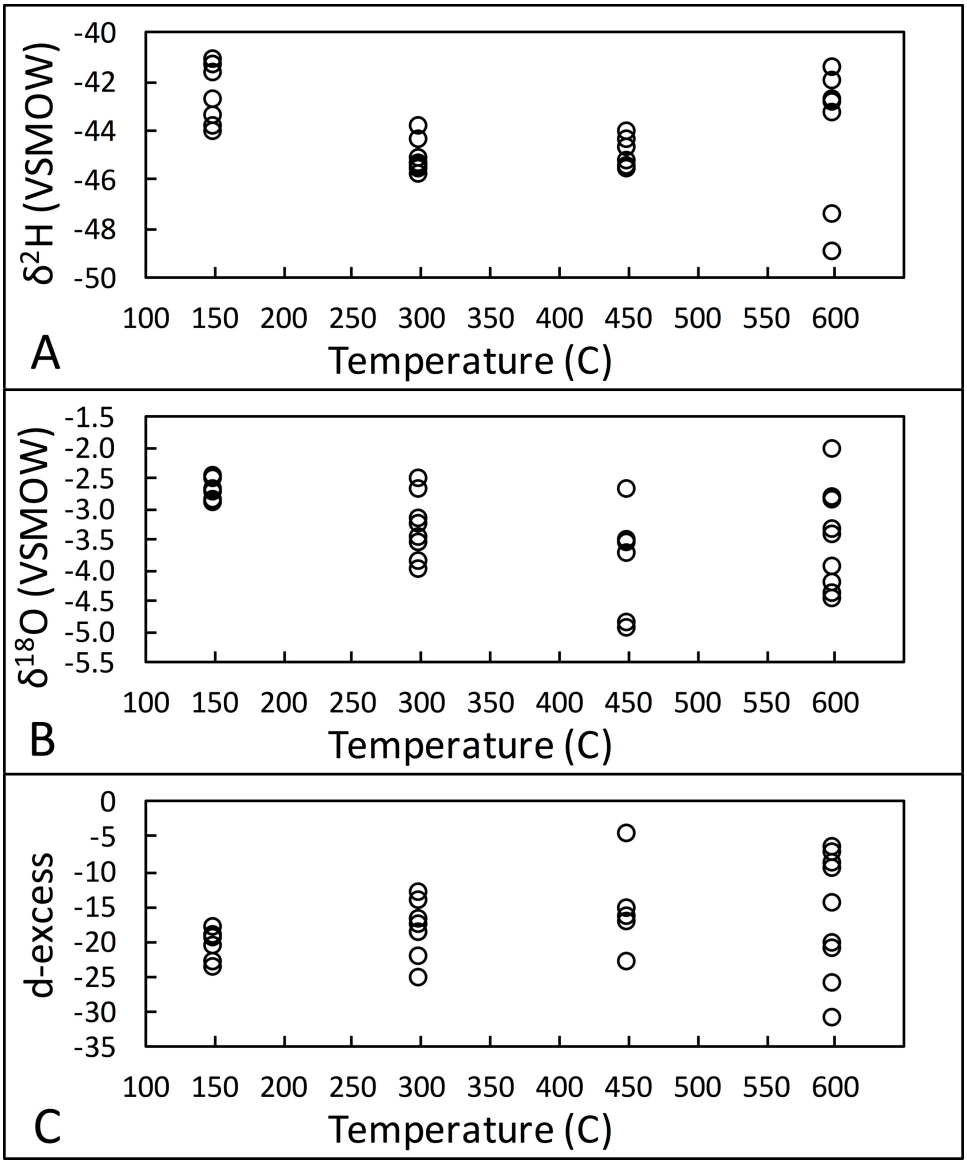

917

918

919

Figure 4

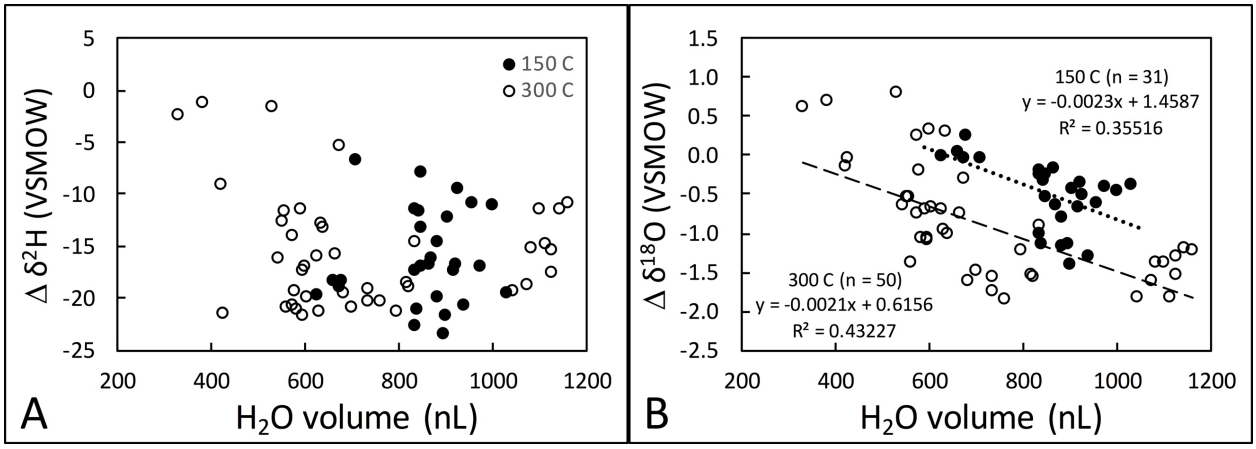
A
Δ δ2H (VSMOW)
H2O volume (nL)
150 C
300 C
B
Δ δ18O (VSMOW)
H2O volume (nL)
150 C (n = 31)
y = -0.0023x + 1.4587
R² = 0.35516
300 C (n = 50)
y = -0.0021x + 0.6156
R² = 0.43227

925 Figure 5

926

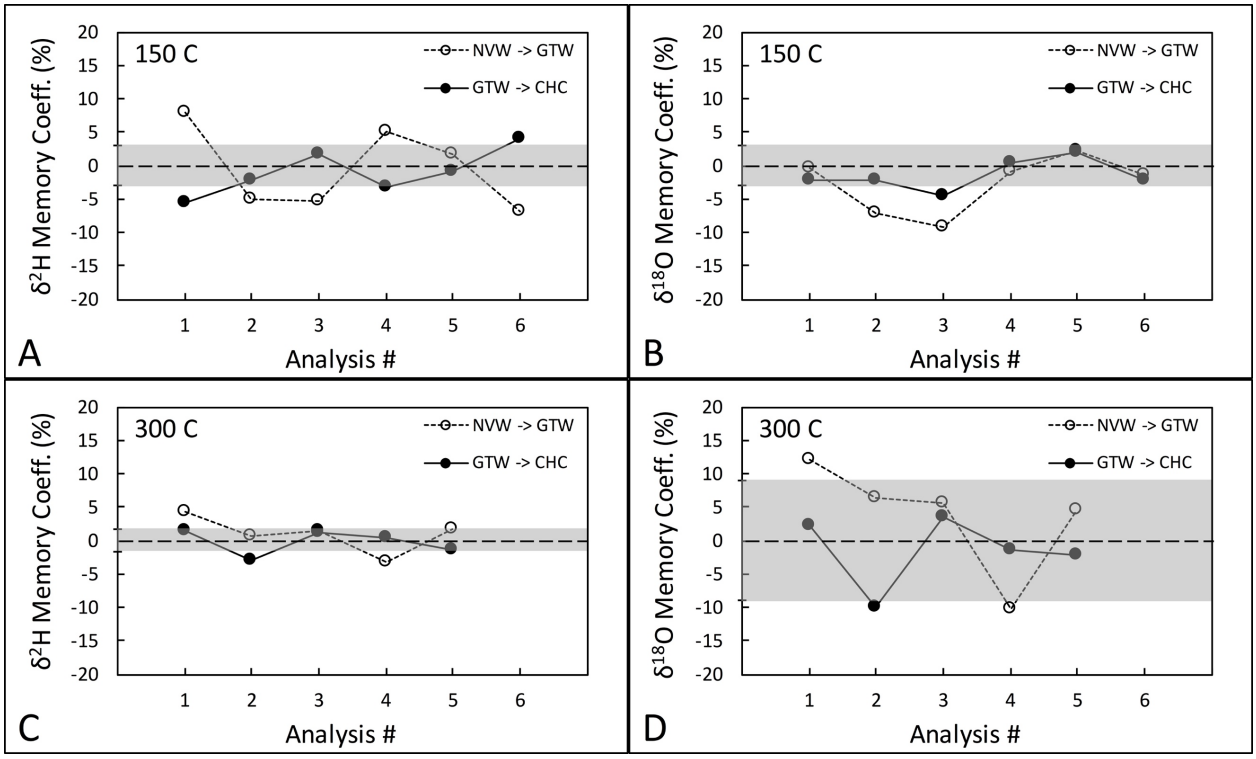

927

928

929

930 Figure 6

931

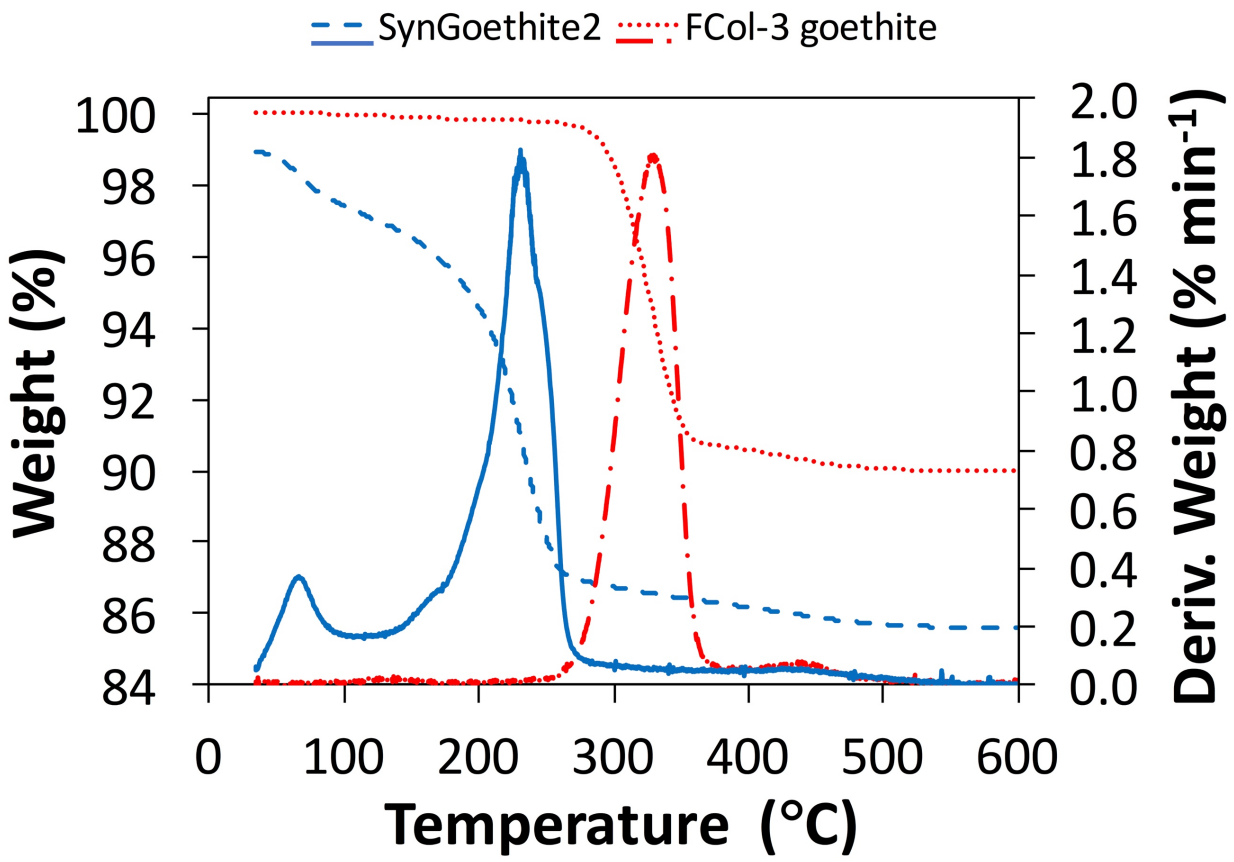

932

933

934

935 Figure 7

936

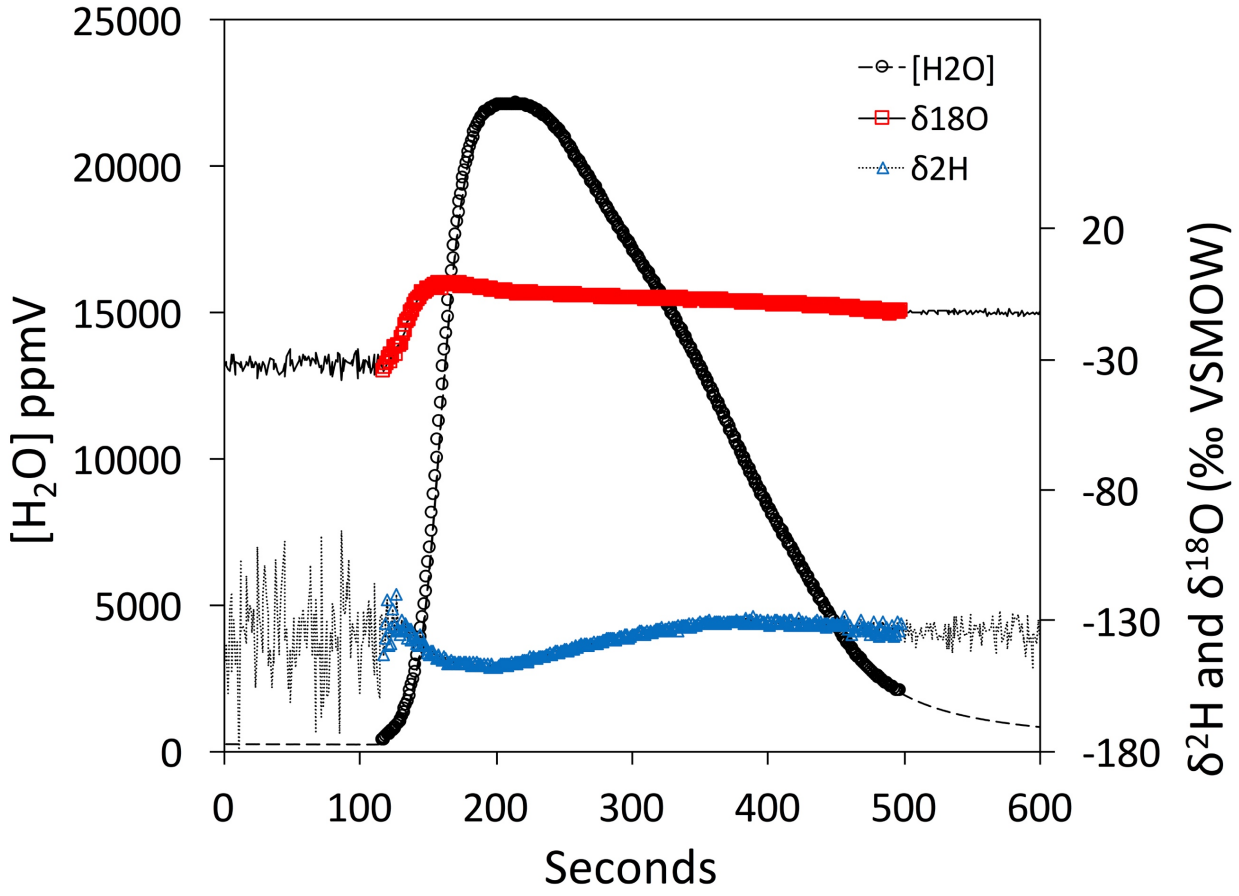

937

938

939

940 Table 1

941

water	δ^2H (‰ VSMOW)	$\delta^{18}O$ (‰ VSMOW)
CHC	-24.4	-2.51
GTW	-70.1	-9.4
NVW	-119.4	-15.11
ATW	-164.3	-20.9

942

943

944

945 Table 2

946

				Source Water			Mineral Hydration Water				
Sample	Locality	Mineral Type	n	δ^2H (‰ VSMOW)	$\delta^{18}O$ (‰ VSMOW)	Analysis Temp (C)	Water Yield (%) (± 1 S.D.)	δ^2H_{OH} (‰ VSMOW) (± 1 S.D.)	$\alpha_{m-w}^{H,OH}$	$\delta^{18}O_{OH}$ (‰ VSMOW) (± 1 S.D.)	$\alpha_{m-w}^{O,OH}$
SynGoethite2	Livermore, California	synthetic goethite	5	-71.0 [a]	-7.8 [a]	280	10.5 (0.04)	-158.2 (1.2)	0.9062	-10.64 (0.17)	0.9972
FCol-3_Goet	Florissant, Colorado	natural goethite	4	-110.0 [b]	-14.9 [c]	370	9.1 (0.03)	-138.2 (0.3)	0.9683	-4.72 (0.32)	1.0103

[a] Source water δ values measured by TGA-IRIS on liquid water samples

[b] Source water δ values from Yapp and Pedley, 1985

947 [c] Source water δ value calculated from δ^2H value (b) using GMWL of Rozanski et al., 1993

948

949